DOI: 10.1002/asia.200900010

Probing the Initial Stages of Molecular Organization of Oligo(*p*-phenylenevinylene) Assemblies with Monolayer Protected Gold Nanoparticles

Vattakattu R. Rajeev Kumar,[a] Vadukumpulli Sajini,[a] Theruvakkattil S. Sreeprasad,[a] Vakayil K. Praveen,[b] Ayyappanpillai Ajayaghosh,[b] and Thalappil Pradeep*[a]

Dedicated to Professor C. N. R. Rao on the occasion of his 75th birthday

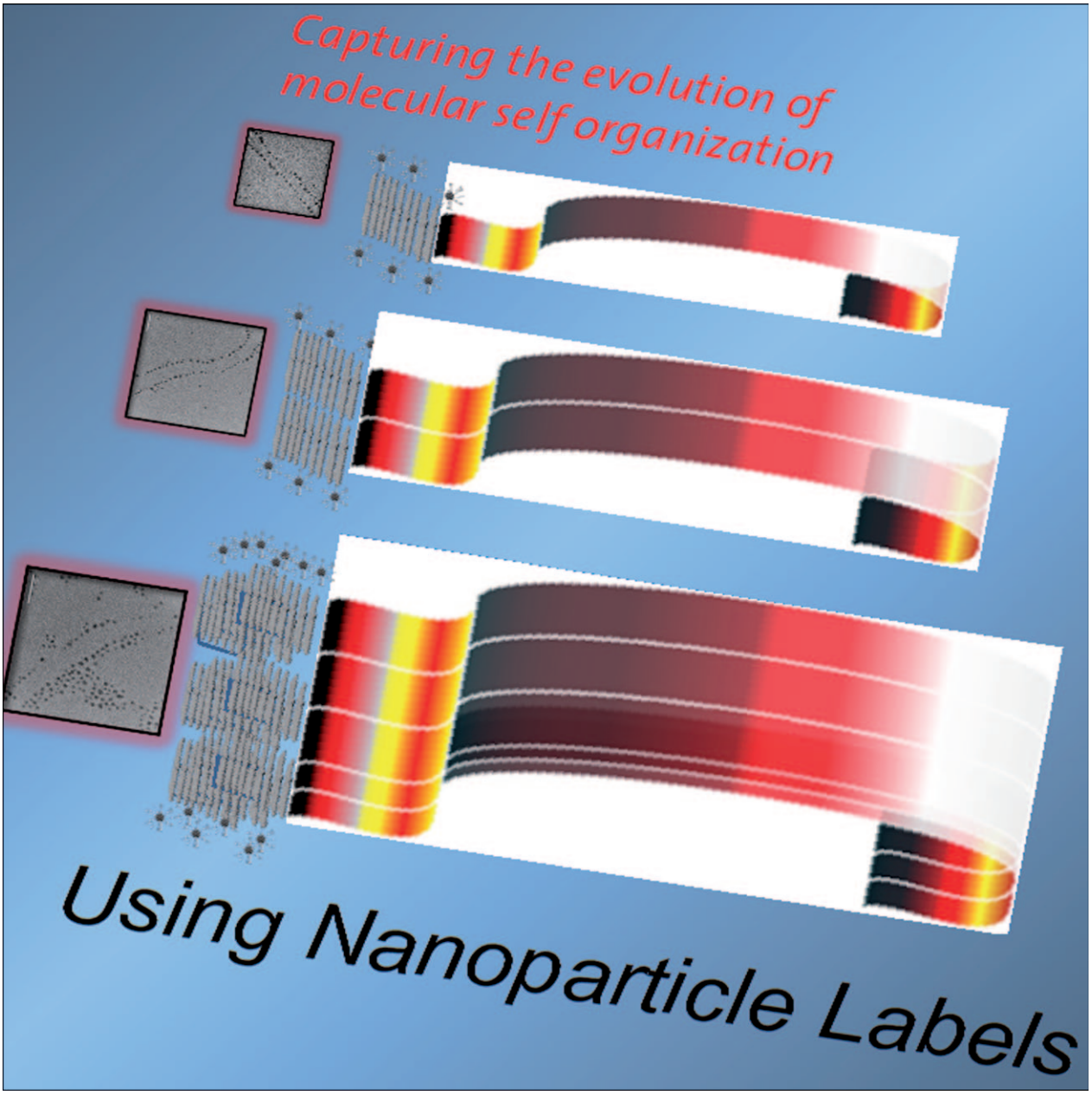

Abstract: Thiol-protected gold nanoparticles (GNPs) have been used to probe the initial stages of the molecular organization of oligo(*p*-phenylenevinylene) (OPV) gelators. The hybrid materials prepared by the self-assembly of OPVs and GNPs are characterized by optical microscopy, fluorescence microscopy, scanning electron microscopy, transmission electron microscopy, and atomic force microscopy. GNPs are located preferentially on the sides of the OPV structures, which implies the presence of alkyl chains at the edges, which makes the assemblies hydrophobic. TEM analyses at the early stages of self-assembly show tapes that have a width of 4 nm, which upon further self-assembly, form fibrils through hydrogen bonding. The experiment was performed with GNPs protected with dodecane and octadecane thiols. The existence of tapes, ribbons, fibrils, and fibers were confirmed by nanoparticle marking. Based on the experimental data, we have proposed a hierarchical model for the self-assembly of OPV molecules. The presence of nanoparticles does not alter the morphology or electronic properties of the OPV structures, as revealed by microscopic and spectroscopic studies.

Keywords: gold · hydrogen bonding · nanoparticles · self-assembly · TEM

Introduction

The self-assembly route, through which nature makes complex structures often involves a hierarchical organization of the building blocks such as proteins and peptides. The rod-shaped collagen fibers, where peptides are hierarchically self-assembled, is an example of such a process.[1] The rod-shaped tobacco mosaic virus is another example of hierarchical self-assembly of protein units, built around the ribonucleic acid (RNA).[2] Such self-assembly has also been displayed by various synthetic molecules. Crown ether appended phthalocyanine is an example of such a molecule.[3] It can self-assemble with the help of weak interactions to give structures with tunable chirality. The hierarchical self-assembly that leads to supramolecular architectures has received considerable attention because of the medical implications; motivation for such studies include the understanding of the molecular mechanism behind life threatening amyloidosis diseases like Alzheimer's. Various attempts have been made to explain how entangled superstructures evolve from such small molecules.[4–6] In the case of peptides, theoretical models that predict the morphology of self-assembled structures, starting from molecular parameters, are available.

Oligo(*p*-phenylenevinylene) (OPV) derivatives form a class of well-known organic semiconductor precursors that have possible applications in devices such as light-emitting diodes and solar cells.[7] The molecule is characterized by an extended π-conjugated system and the chromophore-linked molecular system has a tremendous influence on optical and electronic properties. Molecular recognition driven self-assembly has been used to organize nucleotide-appended OPV into right-handed helical stacks.[8] In one of the reports, OPV was chiraly arranged by placing the molecules on the periphery of urea based foldamers.[9]

The first OPV based organogelator was reported by George and Ajayaghosh.[10] Self-organization of OPVs result in a large shift in emission towards the longer wavelength region, which has been attributed to efficient excitation energy migration within the aggregates.[11] This property of OPV self-assembly makes it an excellent scaffold for energy transfer to suitable acceptors.[12–15] In addition, the self-assembly of OPVs could be biased towards a preferred handedness by the incorporation of chiral handles and through the *sergeant and soldiers* co-assembly.[16,17]

The hybrids of small-molecule gelators with nanoparticles is a relatively new subject area.[18] In order to improve the interaction between the gold nanoparticles (GNPs) and low-molecular-weight gelator fibers, thiol-derivatized gelators have been used instead of the parent compound and the ligand-exchange reaction has been used to decorate the self-assembled fibers with nanoparticles.[19] The self-assembly of

[a] V. R. R. Kumar, V. Sajini,[+] T. S. Sreeprasad, Prof. T. Pradeep
DST Unit on Nanoscience (DST-UNS)
Department of Chemistry
and Sophisticated Analytical Instrument Facility
Indian Institute of Technology Madras
Chennai 600 036 (India)
Fax: (+91) 442-257-0545
E-mail: pradeep@iitm.ac.in

[b] V. K. Praveen, Dr. A. Ajayaghosh
Photosciences and Photonics Group
National Institute for Interdisciplinary Science and Technology
(NIIST), CSIR
Trivandrum 695019 (India)

[+] Current address: Department of Chemistry
National University of Singapore
Singapore 117543 (Singapore)

Supporting information for this article is available on the WWW under http://dx.doi.org/10.1002/asia.200900010.

OPV-functionalized GNP into fractal-like structures was reported recently by Schenning et al.[20] However, it should be pointed out that colloidal gold–organic hybrid systems are much older in the literature. GNPs have been used as markers in electron microscopy in a number of applications, especially biology.[21] There are also very recent initiatives in this direction. Through an antigen–antibody reaction, it is possible to tag the surface of cells with nanoparticles, thereby allowing the determination of the number of receptors on the cell surface. Gold clusters, because of their greater penetration power compared to GNPs, have been used to label organelles, such as microtubules, present inside the cell.[22,23]

However, very few attempts have been made to probe the molecular details of OPV fibers. In one report, GNPs protected with monolayers of thioctic acid-functionalized OPV was used as a probe to understand the molecular structure of the OPV fiber.[24] However, no attempt was made to isolate the primitive form, such as tapes or ribbons, which occurs at the early stages of the self-assembly. Also, molecular details, such as the functional groups present on the surface of the self-assembled structures, are not present in these studies. Herein, we have used alkane thiol-protected GNPs as a probe to study the structure of the gels. The weak interactions through which the nanoparticle probe interacts with the structure may not disturb the self-assembly in the target OPV structure. Indeed, we found that OPV forms the same kinds of structure in the presence of GNPs.

When thiol-protected GNPs are mixed with OPV derivatives, the long hydrocarbon chains of thiols interact with the alkyl chains of the self-assembled supramolecular OPV tapes forming OPV–nanoparticle composites, wherein the nanoparticles decorate the 'surfaces' of the self-assembled OPV structures. We have utilized this aspect in the construction of GNP–OPV composites. The synthesis and characterization of the composites, as well as investigations into the molecular structure of such composites, are the aspects discussed in this paper. The chain length of the thiols was also varied to see their effect on the composite formation. We believe that the supramolecular assemblies of OPVs and nanoparticles could be novel systems with interesting properties for applications in areas such as optoelectronics. Therefore, a study into their molecular structures is relevant and is of current interest.

Results and Discussion

The monolayer protected GNPs used in the study were thoroughly characterized by various microscopic and spectroscopic methods. TEM images of GNPs protected by dodecane (Au@C12) and octadecane thiols (Au@C18) are given in Figure S1 of the Supporting Information. All the nanoparticles are ~3 nm in diameter and are highly monodisperse. The structure of the OPV molecule used for the self-assembly experiments is shown in Figure 1. The molecule contains terminal hydroxy groups, which can participate in hydrogen bonding. The alkyl chains of OPVs can interdigitate among themselves. The presence of benzene rings in the molecule gives the possibility of π–π interactions. An interplay of all these interactions leads to the formation of fibers of 20–200 nm in width and several micrometers in length. A network formed by such entangled fibers allows the structure to hold large amounts of solvent within its cage, to form a gel. The molecule is also characterized by a thermo-reversible sol-gel transition. At 60 °C, in a toluene solution containing 1×10^{-3} M gelator, OPV exists in the dissolved form, whereas at room temperature, it self-assembles to form a gel. Self-assembly has a dramatic influence on the optical and photophysical properties of the molecule.[10,27–29] However, in the concentration window between 10^{-3} and 10^{-4} M, the OPV molecules are expected to form primitive self-assembled structures. These structures, with no distinct spectroscopic features, are seen using TEM with the help of GNP marking. This arises from the alkyl chains of GNPs being able to interdigitate into the OPV structures. We thought that primitive structures, with GNP markings, could be formed when OPV molecules in the dissolved form at 60 °C were to self-assemble upon cooling in the presence of GNPs. We prepared such samples as detailed in the Supporting Information.

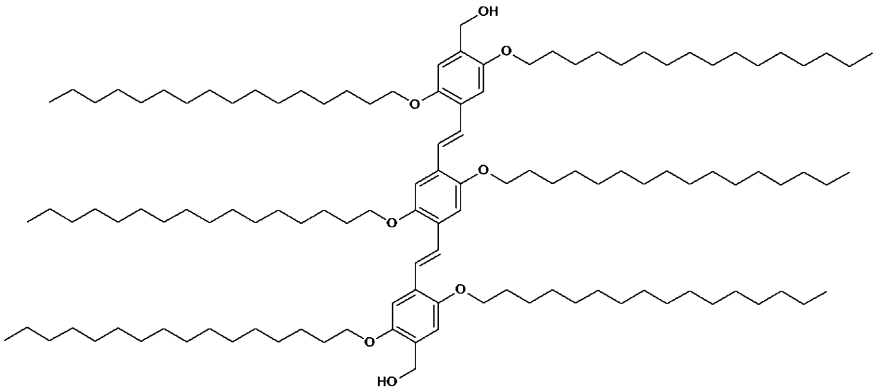

Figure 1. The structure of the OPV molecule used for the self-assembly experiments. Hydrogen bonding, van der Waals interaction, and π–π stacking are the forces believed to play key roles in the self-assembly of the molecule.

Figure 2a shows the optical image of pristine OPV fibers and Figure 2b is that of Au@C12 decorated OPV fibers, prepared at a concentration of 1×10^{-3} M. The presence of simi-

CHEMISTRY
AN ASIAN JOURNAL

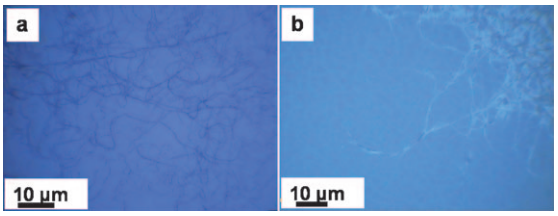

Figure 2. Optical images of OPV fibers (a) and Au@C12 decorated OPV fibers (b). The contrast is not good in the white-light image.

lar fibers in both images indicates that GNPs do not prevent the gelation of the OPV molecule. The gelation of OPV molecules in the presence of nanoparticles has already been reported in the literature.[20] Optical images presented here imply that the structures formed are similar in both cases. The fibers extend over hundreds of micrometers in length. Morphologies of the structures observed in both cases are similar. The sample containing the nanoparticles, showed a greater tendency to form twisted fibers compared to the one without nanoparticles. Molecular details of the fibers were investigated by electron microscopy.

The intense fluorescence of the OPV molecule was used to image the self-assembled fibers. In Figure 3a and 3b, we

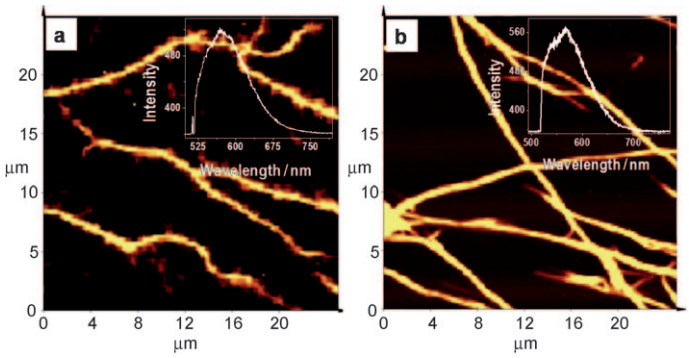

Figure 3. Fluorescence images of OPV fibers (a) and OPV fibers decorated with Au@C12 (b). The insets show the emission spectrum for each sample. The samples were excited with 514.5 nm laser. The scan area is 25×25 μm. The entire fluorescence intensity was used to image the structures.

compare the fluorescence images of the parent OPV fibers and the Au@C12 decorated OPV fibers. The emission spectra from these self-assembled structures are shown in the insets of the figures. The spectra shows a broad fluorescence emission centered around 570 nm. This peak position is comparable to that of the fluorescence of the film sample.[10] The entangled fibers characteristic of the gels are present in the images of both the parent OPV and Au@C12 decorated OPV. The images and spectra suggest that the electronic structures of the OPVs are not disturbed significantly by the presence of the nanoparticles.

The TEM images of OPV and Au@C12 decorated OPV are shown in Figure 4. The solution concentration was 1×10^{-3} M with respect to the OPV molecule. The images fur-

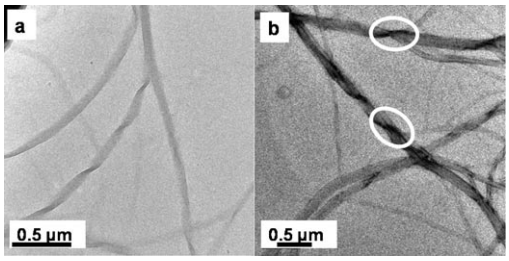

Figure 4. TEM images of OPV fibers (a) and OPV/Au@C12 hybrid (b). The darker areas marked in (b) correspond to twists.

ther support the fact that the nanoparticles do not prevent the molecules from forming the gel. The pitch of OPV fiber was 500 nm whereas that of the GNP decorated OPV fiber was 700 nm. The structures with and without nanoparticles are similar in appearance. One significant difference seen between the images is that the nanoparticle-added fibers are darker and this is especially noticeable at the twists (see the marked regions in Figure 4b). This arises because in those areas, there is larger density of nanoparticles and consequently, a high electron density. The field emission scanning electron microscopy (FE-SEM) images of OPV/Au@C12 composite show the fibers (see Supporting Information, Figure S2). The AFM analysis of OPV showed fibers of 80 nm width and 4 nm height (Figures S3 and S4 of the Supporting Information). All the data suggests that the nanoparticles do not disturb the OPV assemblies in any significant way.

In order to understand the nature of interaction of the nanoparticles with OPV, dispersions that contain self-assembled structures were equilibrated with increasing number of GNPs (see the Experimental Section). The UV/Vis spectrum was recorded after each addition of the nanoparticle solution (containing 2 mg Au@C18 per mL toluene) to the OPV fibers (see Supporting Information, Figure S5). All the samples showed a peak maximum at 407 nm, which corresponds to the OPV molecule apart from the surface plasmon resonance of GNP at 520 nm. The presence of the nanoparticle did not alter the peak positions of the OPV molecule. The same trend was observed in the fluorescence measurements (see Supporting Information, Figure S6). The samples showed peaks at 461 nm and 479 nm, which corresponds to the OPV molecule. The emission maximum was the same for all the solutions but the intensity reduced considerably in the presence of nanoparticles. This strongly supports the fact that GNPs are located on the surface and the electronic interaction between the constituents in the hybrid is weak. The concentration of OPV used was one at which the self-assembled structures will be present in the solution. These structures do not have distinct optical spectroscopic characteristics.

In order to check whether the self-assembly involves the hierarchical organization of the OPV molecule, we made a solution of OPV and Au@C12. The concentration of OPV in the solution was 1×10^{-4} M. From the previous studies, the OPV molecules were not expected to form a gel at this concentration.[27] The TEM of the hybrid material is shown in

Figure 5a. As we can see from the TEM image, the nanoparticles are located on the self-assembled structure preferentially at the edges. In the case of the OPV molecule, the alkyl chains are the only part that can interact with the monolayer protected GNPs. Hence, the structures may be assumed to be formed by the interdigitation of the alkyl chains of the OPV molecule with those of the GNPs. Such interdigitation of alkyl chains has already been observed in monolayer protected GNPs.[30] The width of the self-assembled structure estimated by measuring the distance between the nanoparticles on opposite sides was 4 nm. This is close to the width of the OPV molecules. As there is only a single layer of nanoparticles, the structure observed is of one molecule in thickness. With multiple molecules stacked in the assembly, more than one layer of nanoparticles on either side was expected. We name these structures *tapes*. In order to further see the evolution of the self-assembled structures, GNP–OPV composites were prepared by increasing the amount of OPV in the solution. The TEM image of the hybrid so prepared is shown in Figure 5b. The concentration of the OPV molecule in the solution was 2.5×10^{-4} M. The tapes formed at the beginning of the self-assembly can either increase the thickness, by associating with other tapes through hydrogen bonding, or increase the width, by associating with other tapes through interdigitation of the alkyl chains. The former structures formed by hydrogen bonding, being more than one molecule in thickness, can accommodate multiple layers of nanoparticles on the sides, whereas the latter formed through interdigitation of the alkyl chains, being only single molecule in thickness, can accommodate only a single layer of nanoparticles on either side. The width of the self-assembled structure seen is 8.0 nm, which is twice the width seen at lower OPV concentration. This can happen if the tapes change to *fibrils*, by the interdigitation of the alkyl chains. A single layer of nanoparticles on either side indicates that the structures observed are of one molecule thickness. With multiple molecules, more than one layer of nanoparticles is expected. The OPV/Au@C12 hybrids made by further increasing the OPV concentration to 5×10^{-4} M contained fibrils with a larger width. The TEM image of such a fibril is shown in Figure 5c. The width of the self-assembled structure is 12 nm, which implies that the structure is made of three tapes. This clearly indicates that tapes are the first structure in the hierarchical self-assembly, then come the fibrils. One definite conclusion that comes out from the data is that the self-assembled structures are hydrophobic at the periphery which makes it possible for nanoparticles to interact with them. The widths of the structures observed suggest that the extent of interdigitation seen is small as in the case of nanoparticles.[31]

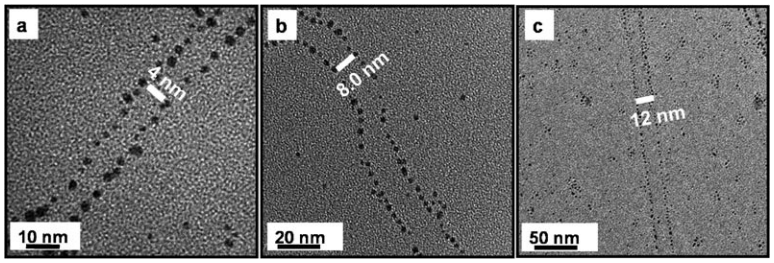

Figure 5. TEM images of OPV tapes at concentrations a) 1×10^{-4} M, b) 2.5×10^{-4} M, and c) 5×10^{-4} M.

The pictorial representation of the self-assembled structures formed at various concentrations is shown in Figure 6. A representation of the tape along with the cross-sectional view, is shown in Figure 6a. The tape is assumed to lie perpendicular to the paper and the electron beam intercepts it from the top. The two dimensional projection of the transmitted electron beam is seen as the TEM image. The width of the self-assembled structure is 4 nm, which indicates that the tape is one molecule in thickness. The π–π stacking results in a self-assembled structure with alkyl chains on either side. The alkyl chains of the gold nanoparticles can interdigitate with such side chains. Upon further increase of the OPV concentration, the OPV tapes formed by the π–π stacking can interdigitate with each other, which results in fibrils with double the width. A pictorial representation of the fibril formed by the interdigitation of the two tapes is shown in Figure 6b. On further increas-

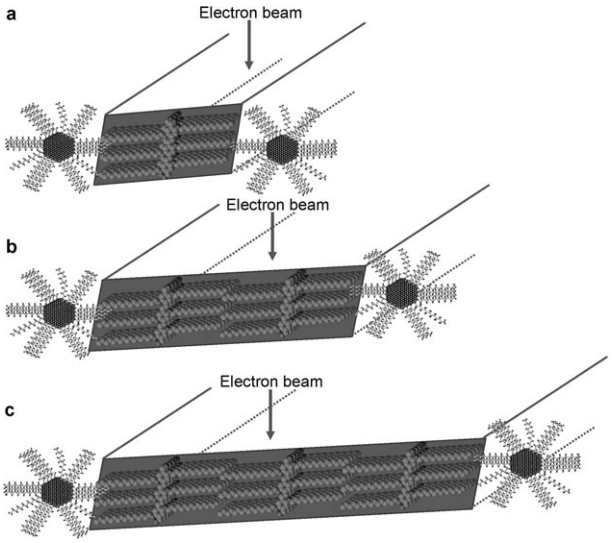

Figure 6. a) Tapes decorated with gold nanoparticles, b) fibrils formed by the interdigitation of two tapes and c) fibrils formed by the interdigitation of three tapes. The interdigitation of the alkyl chains leads to decoration of the structures by gold nanoparticles at the sides. A cross-sectional view (shaded area) of the self-assembled structures is also shown. Lines and the shaded area together represent the tape.

ing the concentration, we obtained fibrils that contain three tapes (Figure 6c).

The last structure in the hierarchical assembly, namely *fibers*, was visible even in the optical microscope. The optical image of the OPV fiber with nanoparticles is shown in Figure 2b. A large area TEM image of the OPV fiber is shown in Figure 7a. The fibers started to form when the concentration of the OPV molecule in the solution reached 10^{-3} M. Any further increase in the OPV concentration leads to gelation. The TEM image of one such OPV fiber is shown in Figure 7b. The circle indicates the junction where a fibril part of the fiber is clearly visible. The width of this fibril, part of a single fiber, is 16 nm (Figure 7c), which implies that it is made up of four tapes. The fibrils could not be part of the fibers because of the nanoparticles located on it. Thus the hierarchical assembly showed that fibrils are made of double, triple, and quadruple tapes, which indicates that the fibrils vary in their width. The presence of fibrils with varying width ultimately results in fibers with varying diameter (see Figure 4b). If the molecule has a chiral center, then the twist created by the chiral center will result in tapes with a definite pitch. As the fibrils formed from such tapes have a definite pitch, it will be difficult for another tape to attach to a growing fibril beyond a certain diameter, because of energy requirements. This will lead to structures with similar diameters, which is not expected for a fiber, made of OPV-like molecules.

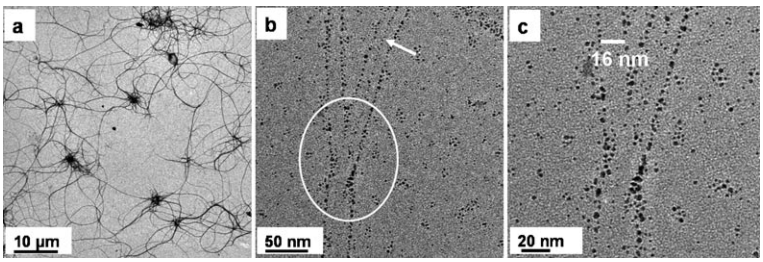

Figure 7. Location of Au@C12 on the fibers. Notice the region marked with circles. A fibril part of the fiber is shown in b and c. The width of the fibril indicates that it is formed from four tapes. The arrow points to the decoration of the fibril with nanoparticles in the middle.

Similar structures were observed with nanoparticles protected with octadecane thiol monolayers. The TEM images of the OPV/Au@C18 hybrid at various stages of self-assembly are shown in Figure 8. The structure observed at the early stage of self-assembly is shown in Figure 8a and 8b. The presence of additional layers of nanoparticles on the sides of the structures indicates that they are tapes with considerable thickness. This also supports the hydrogen bonding of the OPV molecules. The tapes observed in the case of OPV/Au@18 were 5 nm in width. This was expected because of the longer octadecane thiol monolayer that was used to probe the structure. Such a long alkyl chain will increase the distance between the gold core and the tapes.

The fibrils observed upon further increasing the concentration of OPV are shown in Figure 9a and 9b. The fibrils formed were 10 nm in width, which was 2 nm larger than that observed with Au@C12. This indicates that two tapes

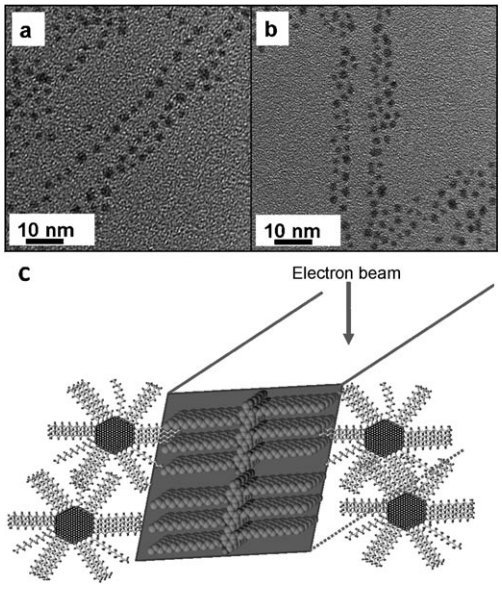

Figure 8. a) and b) Fibrils with Au@C18. c) A schematic cross-sectional view of the self-assembled structure is also given. The nanoparticles are shown as displaced and such displaced nanoparticles in two dimension appear as multiple rows.

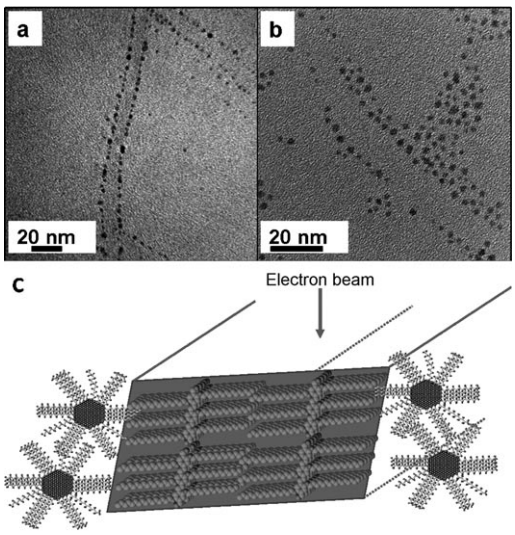

Figure 9. a) and b) TEM images of decorated self-assembled OPV structures with Au@C18 at various magnifications. c) A schematic cross-sectional view of the self-assembled structures is also shown.

are involved in the formation of such a structure. As we can see from the TEM image (Figure 9b), one side of the structure has an additional row of nanoparticles. This can happen if the structure has been formed by the association of tapes with considerable thickness. In that case, the resulting structure will have more sites where the alkyl chains of the nanoparticles can interdigitate. However, as the minimum distance observed between the GNP was around 2 nm, particles do not seem to stack one over the other, which would have appeared as an aggregate in a two-dimensional projection. Even though we have not done detailed investigations on the lower order self-assembled structures by atomic force microscopy, the inter-particle distance observed from TEM measurements showed that the additional layer of nanoparticles is because of the thickness of the self-assembled structures. The inter-particle distance for gold nanoparticles that interdigitate with each other will be different from that of the case where a gold nanoparticle is lying on top of another one. TEM, being a two dimensional projection, creates the impression that they are on the same plane. This scenario is better shown in the SEM images of the fibers. These images clearly show the fibers with multiple layers of nanoparticles on the sides (see Supporting Information, Figure S2).

Based on the experimental data, we propose a hierarchical self-assembly for the OPV molecules. Initially, the OPV molecules form tapes through π–π stacking. The tapes, once formed at a particular concentration, can change to ribbons through hydrogen bonding between the terminal hydroxyl groups. The role of hydrogen bonding in the self-assembly is supported by previous studies on the same molecule.[10,27] Gelling efficiency of OPV was considerably low in hydrogen-bonding solvents such as methanol or when the terminal hydroxyl group was replaced by other groups which do not have the capacity to form hydrogen bonds. The tapes, once formed at a particular concentration, can change to fibrils through hydrogen bonding. This will not change the width of the tapes but would increase the thickness of the tapes as shown by 'structure b' in Figure 10. The fibrils so formed after reaching a definite thickness can further increase the width by interdigitation of the alkyl chains. This leads to the formation of fibrils, represented by 'structure c'. Further self-assembly leads to fibrils with varying width, as shown by 'structure d'. These fibrils are the building block of fibers, shown in Figure 7a. A schematic description of the self-assembly is shown in Figure 10.

The presence of twisted fibers was another important feature exhibited by OPV/gold hybrids. The tapes formed by the π–π stacked OPV molecules, while trying to increase the width by interdigitation, may be forced to adopt a twisted configuration because of the disorder present in the alkyl chain. This may account for the twist observed in the fibers. But such a twist inducted into the tapes by the alkyl chains may not be systematic enough to bring chirality in the system. The TEM images of the OPV/Au@C12 composite at various magnifications are given in Figure 11. A low magnification image of the twisted fibers is shown in Figure 11a. The presence of nanoparticles on curled fibers is clear from the TEM image in Figure 11b.

A cross-sectional view of the tip of the fiber is shown in Figure 12. The π–π stacking is along the length of the fiber.

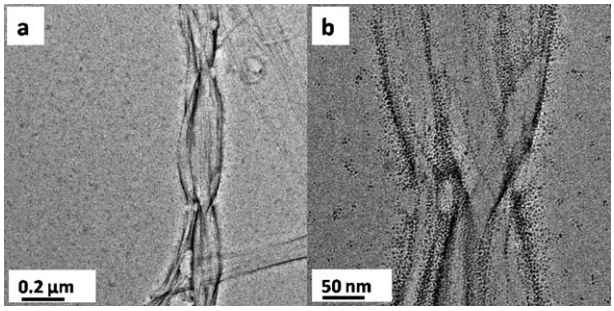

Figure 11. TEM images of OPV/Au@C12 nanocomposite. a) The large area image shows the presence of twisted fibers. b) The decoration of twisted fibers by nanoparticles.

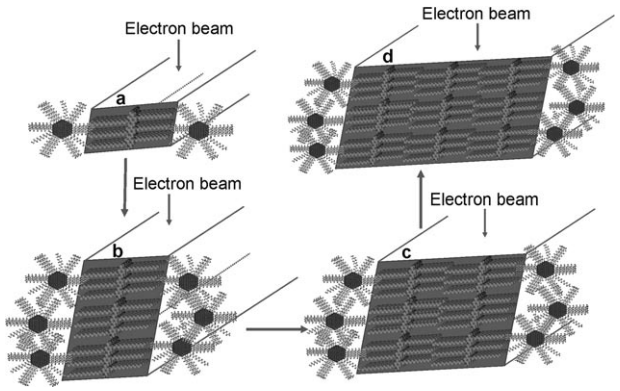

Figure 10. Schematic representation of the hierarchical self-assembly in OPV molecules. The figure shows the cross-sectional view of all the possible self-assembled structures.

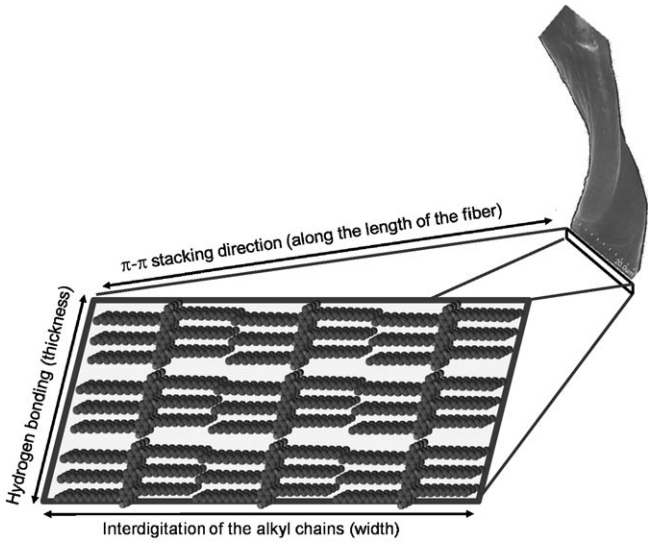

Figure 12. The cross-sectional view of the fiber. The fiber is cut across the length and the cross-sectional view of a single OPV fiber is projected onto a two-dimensional surface. The direction of the π–π stacking, hydrogen bonding, and interdigitation of the alkyl chains of OPV molecules are shown in the picture.

The interdigitation of alkyl chains determines the width of the fiber. The hydrogen bonding between the terminal hydroxyl groups determines the thickness of the fiber. When the thickness is more than one molecule, more than one line of nanoparticles can stack on the sides of the self-assembled structure. In order to avoid confusion, the terms such as length, width, and thickness are marked on the structure which makes the diagram self-explanatory.

Conclusions

Thiol–protected GNPs were used to probe the self-assembly in OPV molecules. The structures formed by the parent OPVs and OPV–nanoparticle mixtures are similar. The self-assembly of OPVs leads to the formation of tapes, which have a width of 4 nm. Further self-assembly results in fibrils, which have nanoparticles on either side. The fibrils further self-assemble to form higher order structures, such as fibers. All the self-assembled structures have alkyl chains on the surface. The studies confirm that the sides of the ribbons are hydrophobic, as proposed earlier. The presence of lower-order structures, such as tapes and fibrils, indicates that self-assembly happens through hierarchical growth in this system. The UV/Vis spectroscopy and fluorescence measurements support weak interactions between the constituents.

Experimental Section

The monolayer protected GNPs were made following the Brust protocol.[25] The synthesis and characterization of OPV has been reported elsewhere.[10,26–29] The nanoparticle/OPV hybrids were made by two methods. As mentioned earlier, at 60 °C in a toluene solution, OPV exists in the dissolved form whereas at room temperature, it self-assembles to form various structures depending on the concentration. In method I, the GNP–OPV hybrids were made by mixing OPV molecules and thiol-capped GNPs in toluene. The mixture was kept at 60 °C for 10 min in an oil bath, then was cooled slowly to room temperature. The amount of OPV molecules in the solution was controlled so that specific structures were formed in the solution.[27] Thus the self-assembled structures were formed in the presence of gold nanoparticles, which decorated the structures. The presence of nanoparticles did not affect the structure and properties of the self-assembly as shown by the data presented. Hybrids were made with dodecane and octadecane thiol-capped GNPs (denoted as Au@C12 and Au@C18). In method II, the nanoparticle/OPV hybrids were prepared by the equilibration of OPV structures with GNPs at room temperature. The OPV structures were prepared with solutions at the required concentrations and nanoparticle dispersions were added to such structures. The nanoparticle addition did not change the OPV concentration significantly as only microliter quantities were added. Thus, it was concluded that the nanoparticles interact with preexisting OPV structures. The nanoparticles themselves do not aggregate at the concentrations used. In order to observe signs of nanoparticle aggregation in TEM and UV/Vis, high concentrations were needed. For uniformity, all the data shown in the main paper and the Supporting Information were collected using samples prepared by method I, except Figures S5 and S6 of the Supporting Information, which used samples prepared by method II. For these measurements, this method was used deliberately as the objective was to see whether electronic interactions exist between nanoparticles and the self-assembled structures. The data showed that no strong electronic interaction exists between the two.

Absorption spectra of the solutions were recorded with a Perkin–Elmer Lambda 25 spectrometer. Transmission electron microscopy (TEM) was recorded with a JEOL-JEM 3010 instrument operating at 300 KeV. The samples were drop-cast on a carbon coated copper grid and were allowed to evaporate under ambient conditions. In general, high energy electron beams damage organic structures and therefore exposures were made for limited periods to minimize structural damage. Examination of the samples for longer duration was done at a reduced energy of 100 KeV. Optical, Raman, and fluorescence images were recorded with a Witec GmbH confocal Raman spectrometer equipped with a 514.5 nm Ar ion laser with a spot size <1 μm. The laser had a maximum power of 40 mW. The excitation laser was focused using a $100\times$ objective and the signal was collected in a back-scattering geometry and guided to a Peltier-cooled charge coupled device (CCD) detector. The sample was mounted on a piezo-equipped scan stage to enable spectral imaging. Single-spot spectra were also acquired using the same grating but with larger integration times. For improved resolution and to ascertain the peak positions, a grating with 1800 grooves/mm was also used while acquiring single-spot spectra. The effective scan range of the spectrometer was 0–9000 cm^{-1} (amounts to a wavelength maximum of 958.2 nm for 514.5 nm excitation), with a decrease in detection efficiency above 750 nm. We have used the Raman microscope to measure the fluorescence image. For spectral imaging, the desired area was partitioned into 10,000 squares (an imaginary 100×100 matrix drawn over it), with each square representing a sampling point and consequently a pixel for the image. Typical signal acquisition time at each pixel of the image was 0.1 s. The intensities of the desired portion of the spectra collected over all the pixels were compared by Scan CTRL Spectroscopy Plus Version 1.32 software, to construct a color-coded image. Spectral intensities acquired over a predefined area were automatically compared to generate color-coded images. In the images, regions coded yellow are with maximum fluorescence intensities and regions shown in black are with minimum signal intensities. Contact mode atomic force microscopy (AFM) measurements were carried out using a reflux coated NANOSENSORS silicon cantilever. The sample was mounted on a piezo-controlled scan stage. A diode laser of wavelength 980 ± 5 nm was used as the beam deflector laser. The movement of the cantilever was detected using a segmented photodiode. Fluorescence measurements were carried out with a JOBIN-YVON Fluorolog model spectrometer. The band pass for excitation and emission was set as 5 nm. Atomic force microscopy (AFM) images were captured with a JEOL JSPM 4210 model instrument. Scanning electron microscopy (SEM) images were acquired using a HITACHI S 4800 FE-SEM instrument.

Acknowledgements

Dr. C. Subramaniam is thanked for the Raman measurements. We would like to acknowledge Dr. A. Sreekumaran Nair, University of Hyogo, Japan for the FE-SEM measurements. T.P. thanks the Department of Science and Technology for supporting his research program on nanomaterials. A.A. is thankful to the Department of Science and Technology for a Ramanna Fellowship.

[1] D. R. Eyre, *Science* **1980**, *207*, 1315–1322.
[2] A. Klug, *Angew. Chem.* **1983**, *95*, 579–596; *Angew. Chem. Int. Ed. Engl.* **1983**, *22*, 565–582.
[3] H. Engelkamp, S. Middelbeek, R. J. M. Nolte, *Science* **1999**, *284*, 785.
[4] A. Aggeli, I. A. Nyrkova, M. Bell, R. Harding, L. Carrick, T. C. B. McLeish, A. N. Semenov, N. Boden, *Proc. Natl. Acad. Sci. USA* **2001**, *98*, 11857.
[5] J. M. Schnur, *Science* **1993**, *262*, 1669.
[6] a) N. Nandi, B. Bagchi, *J. Am. Chem. Soc.* **1996**, *118*, 11208; b) N. Nandi, B. Bagchi, *J. Phys. Chem. A* **1997**, *101*, 1343.

[7] J.-F. Nierengarten, J.-F. Eckert, J.-F. Nicoud, L. Ouali, V. Krasnikov, G. Hadziioannou, *Chem. Commun.* **1999**, 617.
[8] R. Iwaura, F. J. M. Hoeben, M. Masuda, A. P. H. J. Schenning, E. W. Meijer, T. Shimizu, *J. Am. Chem. Soc.* **2006**, *128*, 13298–13304.
[9] R. W. Sinkeldam, F. J. M. Hoeben, M. J. Poouderoijen, I. D. Cat, J. Zhang, S. Furukawa, S. D. Feyter, J. A. J. M. Vekemans, E. W. Meijer, *J. Am. Chem. Soc.* **2006**, *128*, 16113.
[10] S. J. George, A. Ajayaghosh, *J. Am. Chem. Soc.* **2001**, *123*, 5148.
[11] A. Ajayaghosh, S. J. George, V. K. Praveen, *Angew. Chem.* **2003**, *115*, 346; *Angew. Chem. Int. Ed.* **2003**, *42*, 332.
[12] V. K. Praveen, S. J. George, R. Varghese, C. Vijayakumar, A. Ajayaghosh, *J. Am. Chem. Soc.* **2006**, *128*, 7542.
[13] A. Ajayaghosh, C. Vijayakumar, V. K. Praveen, S. S. Babu, R. Varghese, *J. Am. Chem. Soc.* **2006**, *128*, 7174.
[14] A. Ajayaghosh, V. K. Praveen, C. Vijayakumar, S. J. George, *Angew. Chem.* **2007**, *119*, 6376; *Angew. Chem. Int. Ed.* **2007**, *46*, 6260.
[15] A. Ajayaghosh, V. K. Praveen, C. Viyakumar, *Chem. Soc. Rev.* **2008**, *37*, 109.
[16] S. J. George, A. Ajayaghosh, P. Jonkheijm, A. P. H. J. Schenning, E. W. Meijer, *Angew. Chem.* **2004**, *116*, 3504; *Angew. Chem. Int. Ed.* **2004**, *43*, 3422.
[17] A. Ajayaghosh, R. Varghese, S. J. George, C. Vijayakumar, *Angew. Chem.* **2006**, *118*, 1159; *Angew. Chem. Int. Ed.* **2006**, *45*, 1141.
[18] S. Bhat, U. Maitra, *Chem. Mater.* **2006**, *18*, 4224.
[19] M. Kimura, S Kobayashi, T. Kuroda, K. Hanabusa, H. Shirai, *Adv. Mater.* **2004**, *16*, 335.
[20] J. van Herrikhuyzen, R. A. J. Janssen, E. W. Meijer, S. C. J. Meskers, A. P. H. J. Schenning, *J. Am. Chem. Soc.* **2006**, *128*, 686.
[21] a) M. Horisberger, J. Rosset, *J. Histochem. Cytochem.* **1977**, *25*, 295; b) M. A. Hayat, *Colloidal Gold: Principles, Methods and Applications*, *Vol. 1*, Academic Press, San Diego, **1989**; c) M. A. Hayat, *Colloidal Gold: Principles, Methods and Applications*, *Vol. 2*, Academic Press, San Diego, **1989**; d) M. A. Hayat, *Immunogold Silver Staining: Principles, Methods and Applications*, CRC Press, Boca Raton, **1995**.
[22] D. Safer, L. Bolinger, J. S., Jr. Leigh, *J. Inorg. Biochem.* **1986**, *26*, 77.
[23] J. M. Robinson, D. D. Vandre, *J. Histochem. Cytochem.* **1997**, *45*, 631.
[24] J. van Herrikhuyzen, S. J. George, M. R. J. Vos, N. A. J. M. Sommerdijk, A. Ajayaghosh, S. C. J. Meskers, A. P. H. J. Schenning, *Angew. Chem.* **2007**, *119*, 1857–1860; *Angew. Chem. Int. Ed.* **2007**, *46*, 1825–1828.
[25] M. Brust, M. Walker, D. Bethell, D. J. Schffrin, R. Whyman, *J. Chem. Soc. Chem. Commun.* **1994**, 801.
[26] B. Wang, M. R. Wasielewski, *J. Am. Chem. Soc.* **1997**, *119*, 12.
[27] S. J. George, A. Ajayaghosh, *Chem. Eur. J.* **2005**, *11*, 3217.
[28] V. K. Praveen, S. J. George, A. Ajayghosh, *Macromol. Symp.* **2006**, *241*, 1.
[29] A. Ajayaghosh, V. K. Praveen, *Acc. Chem. Res.* **2007**, *40*, 644.
[30] A. C. Templeton, W. P. Wuelfing, R. W. Murray, *Acc. Chem. Res.* **2000**, *33*, 27.
[31] N. Sandhyarani, T. Pradeep, *Int. Rev. Phys. Chem.* **2003**, *22*, 221.

Received: January 8, 2009

